



Measurement of the B^\pm production cross-section in pp collisions at $\sqrt{s} = 7$ TeV

The LHCb collaboration [†]

Abstract

The production of B^\pm mesons in proton-proton collisions at $\sqrt{s} = 7$ TeV is studied using 35 pb^{-1} of data collected by the LHCb detector. The B^\pm mesons are reconstructed exclusively in the $B^\pm \rightarrow J/\psi K^\pm$ mode, with $J/\psi \rightarrow \mu^+ \mu^-$. The differential production cross-section is measured as a function of the B^\pm transverse momentum in the fiducial region $0 < p_T < 40 \text{ GeV}/c$ and with rapidity $2.0 < y < 4.5$. The total cross-section, summing up B^+ and B^- , is measured to be

$$\sigma(pp \rightarrow B^\pm X, 0 < p_T < 40 \text{ GeV}/c, 2.0 < y < 4.5) = 41.4 \pm 1.5 (\text{stat.}) \pm 3.1 (\text{syst.}) \mu\text{b}.$$

Submitted to JHEP

[†] Authors are listed on the following pages.

The LHCb collaboration

R. Aaij³⁸, C. Abellan Beteta^{33,n}, B. Adeva³⁴, M. Adinolfi⁴³, C. Adrover⁶, A. Affolder⁴⁹, Z. Ajaltouni⁵, J. Albrecht³⁵, F. Alessio³⁵, M. Alexander⁴⁸, G. Alkhazov²⁷, P. Alvarez Cartelle³⁴, A.A. Alves Jr²², S. Amato², Y. Amhis³⁶, J. Anderson³⁷, R.B. Appleby⁵¹, O. Aquines Gutierrez¹⁰, F. Archilli^{18,35}, L. Arrabito⁵⁵, A. Artamonov³², M. Artuso^{53,35}, E. Aslanides⁶, G. Auriemma^{22,m}, S. Bachmann¹¹, J.J. Back⁴⁵, D.S. Bailey⁵¹, V. Balagura^{28,35}, W. Baldini¹⁶, R.J. Barlow⁵¹, C. Barschel³⁵, S. Barsuk⁷, W. Barter⁴⁴, A. Bates⁴⁸, C. Bauer¹⁰, Th. Bauer³⁸, A. Bay³⁶, I. Bediaga¹, S. Belogurov²⁸, K. Belous³², I. Belyaev²⁸, E. Ben-Haim⁸, M. Benayoun⁸, G. Bencivenni¹⁸, S. Benson⁴⁷, J. Benton⁴³, R. Bernet³⁷, M.-O. Bettler¹⁷, M. van Beuzekom³⁸, A. Bien¹¹, S. Bifani¹², T. Bird⁵¹, A. Bizzeti^{17,h}, P.M. Bjørnstad⁵¹, T. Blake³⁵, F. Blanc³⁶, C. Blanks⁵⁰, J. Blouw¹¹, S. Blusk⁵³, A. Bobrov³¹, V. Bocci²², A. Bondar³¹, N. Bondar²⁷, W. Bonivento¹⁵, S. Borghi^{48,51}, A. Borgia⁵³, T.J.V. Bowcock⁴⁹, C. Bozzi¹⁶, T. Brambach⁹, J. van den Brand³⁹, J. Bressieux³⁶, D. Brett⁵¹, M. Britsch¹⁰, T. Britton⁵³, N.H. Brook⁴³, H. Brown⁴⁹, K. de Bruyn³⁸, A. Büchler-Germann³⁷, I. Burducea²⁶, A. Bursche³⁷, J. Buytaert³⁵, S. Cadeddu¹⁵, O. Callot⁷, M. Calvi^{20,j}, M. Calvo Gomez^{33,n}, A. Camboni³³, P. Campana^{18,35}, A. Carbone¹⁴, G. Carboni^{21,k}, R. Cardinale^{19,i,35}, A. Cardini¹⁵, L. Carson⁵⁰, K. Carvalho Akiba², G. Casse⁴⁹, M. Cattaneo³⁵, Ch. Cauet⁹, M. Charles⁵², Ph. Charpentier³⁵, N. Chiapolini³⁷, K. Ciba³⁵, X. Cid Vidal³⁴, G. Ciezarek⁵⁰, P.E.L. Clarke^{47,35}, M. Clemencic³⁵, H.V. Cliff⁴⁴, J. Closier³⁵, C. Coca²⁶, V. Coco³⁸, J. Cogan⁶, P. Collins³⁵, A. Comerma-Montells³³, F. Constantin²⁶, A. Contu⁵², A. Cook⁴³, M. Coombes⁴³, G. Corti³⁵, B. Couturier³⁵, G.A. Cowan³⁶, R. Currie⁴⁷, C. D'Ambrosio³⁵, P. David⁸, P.N.Y. David³⁸, I. De Bonis⁴, S. De Capua^{21,k}, M. De Cian³⁷, F. De Lorenzi¹², J.M. De Miranda¹, L. De Paula², P. De Simone¹⁸, D. Decamp⁴, M. Deckenhoff⁹, H. Degaudenzi^{36,35}, L. Del Buono⁸, C. Deplano¹⁵, D. Derkach^{14,35}, O. Deschamps⁵, F. Dettori³⁹, J. Dickens⁴⁴, H. Dijkstra³⁵, P. Diniz Batista¹, F. Domingo Bonal^{33,n}, S. Donleavy⁴⁹, F. Dordei¹¹, A. Dosil Suárez³⁴, D. Dossett⁴⁵, A. Dovbnya⁴⁰, F. Dupertuis³⁶, R. Dzhelyadin³², A. Dziurda²³, S. Easo⁴⁶, U. Egede⁵⁰, V. Egorychev²⁸, S. Eidelman³¹, D. van Eijk³⁸, F. Eisele¹¹, S. Eisenhardt⁴⁷, R. Ekelhof⁹, L. Eklund⁴⁸, Ch. Elsasser³⁷, D. Elsby⁴², D. Esperante Pereira³⁴, A. Falabella^{16,e,14}, E. Fanchini^{20,j}, C. Färber¹¹, G. Fardell⁴⁷, C. Farinelli³⁸, S. Farry¹², V. Fave³⁶, V. Fernandez Albor³⁴, M. Ferro-Luzzi³⁵, S. Filippov³⁰, C. Fitzpatrick⁴⁷, M. Fontana¹⁰, F. Fontanelli^{19,i}, R. Forty³⁵, O. Francisco², M. Frank³⁵, C. Frei³⁵, M. Frosini^{17,f}, S. Furcas²⁰, A. Gallas Torreira³⁴, D. Galli^{14,c}, M. Gandelman², P. Gandini⁵², Y. Gao³, J.-C. Garnier³⁵, J. Garofoli⁵³, J. Garra Tico⁴⁴, L. Garrido³³, D. Gascon³³, C. Gaspar³⁵, R. Gauld⁵², N. Gauvin³⁶, M. Gersabeck³⁵, T. Gershon^{45,35}, Ph. Ghez⁴, V. Gibson⁴⁴, V.V. Gligorov³⁵, C. Göbel⁵⁴, D. Golubkov²⁸, A. Golutvin^{50,28,35}, A. Gomes², H. Gordon⁵², M. Grabalosa Gándara³³, R. Graciani Diaz³³, L.A. Granado Cardoso³⁵, E. Graugés³³, G. Graziani¹⁷, A. Grecu²⁶, E. Greening⁵², S. Gregson⁴⁴, B. Gui⁵³, E. Gushchin³⁰, Yu. Guz³², T. Gys³⁵, C. Hadjivasiliou⁵³, G. Haefeli³⁶, C. Haen³⁵, S.C. Haines⁴⁴, T. Hampson⁴³, S. Hansmann-Menzemer¹¹, R. Harji⁵⁰, N. Harnew⁵², J. Harrison⁵¹, P.F. Harrison⁴⁵, T. Hartmann⁵⁶, J. He⁷, V. Heijne³⁸, K. Hennessy⁴⁹, P. Henrard⁵, J.A. Hernando Morata³⁴, E. van Herwijnen³⁵, E. Hicks⁴⁹, K. Holubyev¹¹, P. Hopchev⁴, W. Hulsbergen³⁸, P. Hunt⁵², T. Huse⁴⁹, R.S. Huston¹², D. Hutchcroft⁴⁹, D. Hynds⁴⁸,

V. Iakovenko⁴¹, P. Ilten¹², J. Imong⁴³, R. Jacobsson³⁵, A. Jaeger¹¹, M. Jahjah Hussein⁵,
 E. Jans³⁸, F. Jansen³⁸, P. Jatou³⁶, B. Jean-Marie⁷, F. Jing³, M. John⁵², D. Johnson⁵²,
 C.R. Jones⁴⁴, B. Jost³⁵, M. Kaballo⁹, S. Kandybei⁴⁰, M. Karacson³⁵, T.M. Karbach⁹,
 J. Keaveney¹², I.R. Kenyon⁴², U. Kerzel³⁵, T. Ketel³⁹, A. Keune³⁶, B. Khanji⁶, Y.M. Kim⁴⁷,
 M. Knecht³⁶, R.F. Koopman³⁹, P. Koppenburg³⁸, M. Korolev²⁹, A. Kozlinskiy³⁸,
 L. Kravchuk³⁰, K. Kreplin¹¹, M. Kreps⁴⁵, G. Krocker¹¹, P. Krokovny¹¹, F. Kruse⁹,
 K. Kruzelecki³⁵, M. Kucharczyk^{20,23,35,j}, T. Kvaratskheliya^{28,35}, V.N. La Thi³⁶,
 D. Lacarrere³⁵, G. Lafferty⁵¹, A. Lai¹⁵, D. Lambert⁴⁷, R.W. Lambert³⁹, E. Lanciotti³⁵,
 G. Lanfranchi¹⁸, C. Langenbruch¹¹, T. Latham⁴⁵, C. Lazzeroni⁴², R. Le Gac⁶,
 J. van Leerdam³⁸, J.-P. Lees⁴, R. Lefèvre⁵, A. Leflat^{29,35}, J. Lefrançois⁷, O. Leroy⁶,
 T. Lesiak²³, L. Li³, L. Li Gioi⁵, M. Lieng⁹, M. Liles⁴⁹, R. Lindner³⁵, C. Linn¹¹, B. Liu³,
 G. Liu³⁵, J. von Loeben²⁰, J.H. Lopes², E. Lopez Asamar³³, N. Lopez-March³⁶, H. Lu³,
 J. Luisier³⁶, A. Mac Raighne⁴⁸, F. Machefert⁷, I.V. Machikhiliyan^{4,28}, F. Maciuc¹⁰,
 O. Maev^{27,35}, J. Magnin¹, S. Malde⁵², R.M.D. Mamunur³⁵, G. Manca^{15,d}, G. Mancinelli⁶,
 N. Mangiafave⁴⁴, U. Marconi¹⁴, R. Märki³⁶, J. Marks¹¹, G. Martellotti²², A. Martens⁸,
 L. Martín⁵², A. Martín Sánchez⁷, D. Martínez Santos³⁵, A. Massafferri¹, Z. Mathe¹²,
 C. Matteuzzi²⁰, M. Matveev²⁷, E. Maurice⁶, B. Maynard⁵³, A. Mazurov^{16,30,35},
 G. McGregor⁵¹, R. McNulty¹², M. Meissner¹¹, M. Merk³⁸, J. Merkel⁹, R. Messi^{21,k},
 S. Miglioranza³⁵, D.A. Milanes¹³, M.-N. Minard⁴, J. Molina Rodriguez⁵⁴, S. Monteil⁵,
 D. Moran¹², P. Morawski²³, R. Mountain⁵³, I. Mous³⁸, F. Muheim⁴⁷, K. Müller³⁷,
 R. Muresan²⁶, B. Muryn²⁴, B. Muster³⁶, M. Musy³³, J. Mylroie-Smith⁴⁹, P. Naik⁴³,
 T. Nakada³⁶, R. Nandakumar⁴⁶, I. Nasteva¹, M. Nedos⁹, M. Needham⁴⁷, N. Neufeld³⁵,
 A.D. Nguyen³⁶, C. Nguyen-Mau^{36,o}, M. Nicol⁷, V. Niess⁵, N. Nikitin²⁹, A. Nomerotski^{52,35},
 A. Novoselov³², A. Oblakowska-Mucha²⁴, V. Obraztsov³², S. Oggero³⁸, S. Ogilvy⁴⁸,
 O. Okhrimenko⁴¹, R. Oldeman^{15,d,35}, M. Orlandea²⁶, J.M. Otalora Goicochea², P. Owen⁵⁰,
 K. Pal⁵³, J. Palacios³⁷, A. Palano^{13,b}, M. Palutan¹⁸, J. Panman³⁵, A. Papanestis⁴⁶,
 M. Pappagallo⁴⁸, C. Parkes⁵¹, C.J. Parkinson⁵⁰, G. Passaleva¹⁷, G.D. Patel⁴⁹, M. Patel⁵⁰,
 S.K. Paterson⁵⁰, G.N. Patrick⁴⁶, C. Patrignani^{19,i}, C. Pavel-Nicorescu²⁶, A. Pazos Alvarez³⁴,
 A. Pellegrino³⁸, G. Penso^{22,l}, M. Pepe Altarelli³⁵, S. Perazzini^{14,c}, D.L. Perego^{20,j},
 E. Perez Trigo³⁴, A. Pérez-Calero Yzquierdo³³, P. Perret⁵, M. Perrin-Terrin⁶, G. Pessina²⁰,
 A. Petrella^{16,35}, A. Petrolini^{19,i}, A. Phan⁵³, E. Picatoste Olloqui³³, B. Pie Valls³³, B. Pietrzyk⁴,
 T. Pilar⁴⁵, D. Pinci²², R. Plackett⁴⁸, S. Playfer⁴⁷, M. Plo Casasus³⁴, G. Polok²³,
 A. Poluektov^{45,31}, E. Polcarpo², D. Popov¹⁰, B. Popovici²⁶, C. Potterat³³, A. Powell⁵²,
 J. Prisciandaro³⁶, V. Pugatch⁴¹, A. Puig Navarro³³, W. Qian⁵³, J.H. Rademacker⁴³,
 B. Rakotomiamanana³⁶, M.S. Rangel², I. Raniuk⁴⁰, G. Raven³⁹, S. Redford⁵², M.M. Reid⁴⁵,
 A.C. dos Reis¹, S. Ricciardi⁴⁶, A. Richards⁵⁰, K. Rinnert⁴⁹, D.A. Roa Romero⁵, P. Robbe⁷,
 E. Rodrigues^{48,51}, F. Rodrigues², P. Rodriguez Perez³⁴, G.J. Rogers⁴⁴, S. Roiser³⁵,
 V. Romanovsky³², M. Rosello^{33,n}, J. Rouvinet³⁶, T. Ruf³⁵, H. Ruiz³³, G. Sabatino^{21,k},
 J.J. Saborido Silva³⁴, N. Sagidova²⁷, P. Sail⁴⁸, B. Saitta^{15,d}, C. Salzmann³⁷, M. Sannino^{19,i},
 R. Santacesaria²², C. Santamarina Rios³⁴, R. Santinelli³⁵, E. Santovetti^{21,k}, M. Sapunov⁶,
 A. Sarti^{18,l}, C. Satriano^{22,m}, A. Satta²¹, M. Savrie^{16,e}, D. Savrina²⁸, P. Schaack⁵⁰,
 M. Schiller³⁹, S. Schleich⁹, M. Schlupp⁹, M. Schmelling¹⁰, B. Schmidt³⁵, O. Schneider³⁶,
 A. Schopper³⁵, M.-H. Schune⁷, R. Schwemmer³⁵, B. Sciascia¹⁸, A. Sciubba^{18,l}, M. Seco³⁴,

A. Semennikov²⁸, K. Senderowska²⁴, I. Sepp⁵⁰, N. Serra³⁷, J. Serrano⁶, P. Seyfert¹¹, M. Shapkin³², I. Shapoval^{40,35}, P. Shatalov²⁸, Y. Shcheglov²⁷, T. Shears⁴⁹, L. Shekhtman³¹, O. Shevchenko⁴⁰, V. Shevchenko²⁸, A. Shires⁵⁰, R. Silva Coutinho⁴⁵, T. Skwarnicki⁵³, N.A. Smith⁴⁹, E. Smith^{52,46}, K. Sobczak⁵, F.J.P. Soler⁴⁸, A. Solomin⁴³, F. Soomro^{18,35}, B. Souza De Paula², B. Spaan⁹, A. Sparkes⁴⁷, P. Spradlin⁴⁸, F. Stagni³⁵, S. Stahl¹¹, O. Steinkamp³⁷, S. Stoica²⁶, S. Stone^{53,35}, B. Storaci³⁸, M. Straticiuc²⁶, U. Straumann³⁷, V.K. Subbiah³⁵, S. Swientek⁹, M. Szczekowski²⁵, P. Szczypka³⁶, T. Szumlak²⁴, S. T’Jampens⁴, E. Teodorescu²⁶, F. Teubert³⁵, C. Thomas⁵², E. Thomas³⁵, J. van Tilburg¹¹, V. Tisserand⁴, M. Tobin³⁷, S. Topp-Joergensen⁵², N. Torr⁵², E. Tournefier^{4,50}, S. Tourneur³⁶, M.T. Tran³⁶, A. Tsaregorodtsev⁶, N. Tuning³⁸, M. Ubeda Garcia³⁵, A. Ukleja²⁵, P. Urquijo⁵³, U. Uwer¹¹, V. Vagnoni¹⁴, G. Valenti¹⁴, R. Vazquez Gomez³³, P. Vazquez Regueiro³⁴, S. Vecchi¹⁶, J.J. Velthuis⁴³, M. Veltri^{17,g}, B. Viaud⁷, I. Videau⁷, D. Vieira², X. Vilasis-Cardona^{33,n}, J. Visniakov³⁴, A. Vollhardt³⁷, D. Volyanskyy¹⁰, D. Voong⁴³, A. Vorobyev²⁷, H. Voss¹⁰, S. Wandernoth¹¹, J. Wang⁵³, D.R. Ward⁴⁴, N.K. Watson⁴², A.D. Webber⁵¹, D. Websdale⁵⁰, M. Whitehead⁴⁵, D. Wiedner¹¹, L. Wiggers³⁸, G. Wilkinson⁵², M.P. Williams^{45,46}, M. Williams⁵⁰, F.F. Wilson⁴⁶, J. Wishahi⁹, M. Witek²³, W. Witzeling³⁵, S.A. Wotton⁴⁴, K. Wyllie³⁵, Y. Xie⁴⁷, F. Xing⁵², Z. Xing⁵³, Z. Yang³, R. Young⁴⁷, O. Yushchenko³², M. Zangoli¹⁴, M. Zavertyaev^{10,a}, F. Zhang³, L. Zhang⁵³, W.C. Zhang¹², Y. Zhang³, A. Zhelezov¹¹, L. Zhong³, A. Zvyagin³⁵.

¹Centro Brasileiro de Pesquisas Físicas (CBPF), Rio de Janeiro, Brazil

²Universidade Federal do Rio de Janeiro (UFRJ), Rio de Janeiro, Brazil

³Center for High Energy Physics, Tsinghua University, Beijing, China

⁴LAPP, Université de Savoie, CNRS/IN2P3, Annecy-Le-Vieux, France

⁵Clermont Université, Université Blaise Pascal, CNRS/IN2P3, LPC, Clermont-Ferrand, France

⁶CPPM, Aix-Marseille Université, CNRS/IN2P3, Marseille, France

⁷LAL, Université Paris-Sud, CNRS/IN2P3, Orsay, France

⁸LPNHE, Université Pierre et Marie Curie, Université Paris Diderot, CNRS/IN2P3, Paris, France

⁹Fakultät Physik, Technische Universität Dortmund, Dortmund, Germany

¹⁰Max-Planck-Institut für Kernphysik (MPIK), Heidelberg, Germany

¹¹Physikalisches Institut, Ruprecht-Karls-Universität Heidelberg, Heidelberg, Germany

¹²School of Physics, University College Dublin, Dublin, Ireland

¹³Sezione INFN di Bari, Bari, Italy

¹⁴Sezione INFN di Bologna, Bologna, Italy

¹⁵Sezione INFN di Cagliari, Cagliari, Italy

¹⁶Sezione INFN di Ferrara, Ferrara, Italy

¹⁷Sezione INFN di Firenze, Firenze, Italy

¹⁸Laboratori Nazionali dell’INFN di Frascati, Frascati, Italy

¹⁹Sezione INFN di Genova, Genova, Italy

²⁰Sezione INFN di Milano Bicocca, Milano, Italy

²¹Sezione INFN di Roma Tor Vergata, Roma, Italy

²²Sezione INFN di Roma La Sapienza, Roma, Italy

²³Henryk Niewodniczanski Institute of Nuclear Physics Polish Academy of Sciences, Kraków, Poland

²⁴AGH University of Science and Technology, Kraków, Poland

²⁵Soltan Institute for Nuclear Studies, Warsaw, Poland

²⁶Horia Hulubei National Institute of Physics and Nuclear Engineering, Bucharest-Magurele, Romania

²⁷Petersburg Nuclear Physics Institute (PNPI), Gatchina, Russia

²⁸Institute of Theoretical and Experimental Physics (ITEP), Moscow, Russia

- ²⁹*Institute of Nuclear Physics, Moscow State University (SINP MSU), Moscow, Russia*
- ³⁰*Institute for Nuclear Research of the Russian Academy of Sciences (INR RAN), Moscow, Russia*
- ³¹*Budker Institute of Nuclear Physics (SB RAS) and Novosibirsk State University, Novosibirsk, Russia*
- ³²*Institute for High Energy Physics (IHEP), Protvino, Russia*
- ³³*Universitat de Barcelona, Barcelona, Spain*
- ³⁴*Universidad de Santiago de Compostela, Santiago de Compostela, Spain*
- ³⁵*European Organization for Nuclear Research (CERN), Geneva, Switzerland*
- ³⁶*Ecole Polytechnique Fédérale de Lausanne (EPFL), Lausanne, Switzerland*
- ³⁷*Physik-Institut, Universität Zürich, Zürich, Switzerland*
- ³⁸*Nikhef National Institute for Subatomic Physics, Amsterdam, The Netherlands*
- ³⁹*Nikhef National Institute for Subatomic Physics and Vrije Universiteit, Amsterdam, The Netherlands*
- ⁴⁰*NSC Kharkiv Institute of Physics and Technology (NSC KIPT), Kharkiv, Ukraine*
- ⁴¹*Institute for Nuclear Research of the National Academy of Sciences (KINR), Kyiv, Ukraine*
- ⁴²*University of Birmingham, Birmingham, United Kingdom*
- ⁴³*H.H. Wills Physics Laboratory, University of Bristol, Bristol, United Kingdom*
- ⁴⁴*Cavendish Laboratory, University of Cambridge, Cambridge, United Kingdom*
- ⁴⁵*Department of Physics, University of Warwick, Coventry, United Kingdom*
- ⁴⁶*STFC Rutherford Appleton Laboratory, Didcot, United Kingdom*
- ⁴⁷*School of Physics and Astronomy, University of Edinburgh, Edinburgh, United Kingdom*
- ⁴⁸*School of Physics and Astronomy, University of Glasgow, Glasgow, United Kingdom*
- ⁴⁹*Oliver Lodge Laboratory, University of Liverpool, Liverpool, United Kingdom*
- ⁵⁰*Imperial College London, London, United Kingdom*
- ⁵¹*School of Physics and Astronomy, University of Manchester, Manchester, United Kingdom*
- ⁵²*Department of Physics, University of Oxford, Oxford, United Kingdom*
- ⁵³*Syracuse University, Syracuse, NY, United States*
- ⁵⁴*Pontifícia Universidade Católica do Rio de Janeiro (PUC-Rio), Rio de Janeiro, Brazil, associated to ²*
- ⁵⁵*CC-IN2P3, CNRS/IN2P3, Lyon-Villeurbanne, France, associated member*
- ⁵⁶*Physikalisches Institut, Universität Rostock, Rostock, Germany, associated to ¹¹*

^a*P.N. Lebedev Physical Institute, Russian Academy of Science (LPI RAS), Moscow, Russia*

^b*Università di Bari, Bari, Italy*

^c*Università di Bologna, Bologna, Italy*

^d*Università di Cagliari, Cagliari, Italy*

^e*Università di Ferrara, Ferrara, Italy*

^f*Università di Firenze, Firenze, Italy*

^g*Università di Urbino, Urbino, Italy*

^h*Università di Modena e Reggio Emilia, Modena, Italy*

ⁱ*Università di Genova, Genova, Italy*

^j*Università di Milano Bicocca, Milano, Italy*

^k*Università di Roma Tor Vergata, Roma, Italy*

^l*Università di Roma La Sapienza, Roma, Italy*

^m*Università della Basilicata, Potenza, Italy*

ⁿ*LIFAELS, La Salle, Universitat Ramon Llull, Barcelona, Spain*

^o*Hanoi University of Science, Hanoi, Viet Nam*

1 Introduction

The study of the $b\bar{b}$ production cross-section is a powerful test of perturbative quantum chromodynamics (pQCD) calculations. These are available at next-to-leading order (NLO) [1] and with the fixed-order plus next-to-leading logarithms (FONLL) [2, 3] approximations. In the NLO and FONLL calculations, the theoretical predictions have large uncertainties arising from the choice of the renormalisation and factorisation scales and the b -quark mass [4]. Accurate measurements provide tests of the validity of the different production models. Recently, the LHCb collaboration measured the $b\bar{b}$ production cross-section in hadron collisions using J/ψ from b decays [5] and $b \rightarrow D\mu X$ decays [6]. The two most recent measurements of the B^\pm production cross-section in hadron collisions have been performed by the CDF collaboration in the range $p_T > 6 \text{ GeV}/c$ and $|y| < 1$ [7], where p_T is the transverse momentum and y is rapidity, and by the CMS collaboration in the range $p_T > 5 \text{ GeV}/c$ and $|y| < 2.4$ [8]. This paper presents a measurement of the B^\pm production cross-section in pp collisions at a centre-of-mass energy of $\sqrt{s} = 7 \text{ TeV}$ using $34.6 \pm 1.2 \text{ pb}^{-1}$ of data collected by the LHCb detector in 2010. The B^\pm mesons are reconstructed exclusively in the $B^\pm \rightarrow J/\psi K^\pm$ mode, with $J/\psi \rightarrow \mu^+ \mu^-$. Both the total production cross-section and the differential cross-section, $d\sigma/dp_T$, as a function of the B^\pm transverse momentum for $0 < p_T < 40 \text{ GeV}/c$ and $2.0 < y < 4.5$, are measured.

The LHCb detector [9] is a single-arm forward spectrometer covering the pseudo-rapidity range $2 < \eta < 5$, designed for the study of particles containing b or c quarks. The detector includes a high precision tracking system consisting of a silicon-strip vertex detector surrounding the pp interaction region, a large-area silicon-strip detector located upstream of a dipole magnet with a bending power of about 4 Tm , and three stations of silicon-strip detectors and straw drift-tubes placed downstream. The combined tracking system has a momentum resolution $\Delta p/p$ that varies from 0.4% at $5 \text{ GeV}/c$ to 0.6% at $100 \text{ GeV}/c$, and an impact parameter resolution of $20 \mu\text{m}$ for tracks with high transverse momentum. Charged hadrons are identified using two ring-imaging Cherenkov detectors. Photon, electron and hadron candidates are identified by a calorimeter system consisting of scintillating-pad and pre-shower detectors, an electromagnetic calorimeter and a hadronic calorimeter. Muons are identified by a muon system composed of alternating layers of iron and multiwire proportional chambers.

The LHCb detector uses a two-level trigger system, the first level (L0) is hardware based, and the second level is software based high level trigger (HLT). Here only the triggers used in this analysis are described. At the L0 either a single muon candidate with p_T larger than $1.4 \text{ GeV}/c$ or a pair of muon candidates, one with p_T larger than $0.56 \text{ GeV}/c$ and the other with p_T larger than $0.48 \text{ GeV}/c$, is required. Events passing these requirements are read out and sent to an event filter farm for further selection. In the first stage of the HLT, events satisfying one of the following three selections are kept: the first one confirms the single-muon candidates from L0 and applies a harder p_T selection at $1.8 \text{ GeV}/c$; the second one confirms the single-muon from L0 and looks for another muon in the event, and the third one confirms the dimuon candidates from L0. Both the second and third selections require the dimuon invariant mass to be greater than $2.5 \text{ GeV}/c^2$. The second stage of the HLT selects events that pass any selections of previous stage and contain two muon candidates with an invariant mass within $120 \text{ MeV}/c^2$ of the known J/ψ mass. To reject high-multiplicity events with a large number of pp interactions,

a set of global event cuts (GEC) is applied on the hit multiplicities of sub-detectors.

2 Event selection

Candidates for $J/\psi \rightarrow \mu^+ \mu^-$ decay are formed from pairs of particles with opposite charge. Both particles are required to have a good track fit quality ($\chi^2/\text{ndf} < 4$, where ndf represents the number of degrees of freedom in the fit), a transverse momentum $p_T > 0.7 \text{ GeV}/c$ and to be identified as a muon. In addition, the muon pair is required to originate from a common vertex ($\chi^2/\text{ndf} < 9$). The mass of the reconstructed J/ψ is required to be in the range $3.04 - 3.14 \text{ GeV}/c^2$.

The bachelor kaon candidates used to form $B^\pm \rightarrow J/\psi K^\pm$ candidates are required to have p_T larger than $0.5 \text{ GeV}/c$ and to have a good track fit quality ($\chi^2/\text{ndf} < 4$). No particle identification is used in the selection of the kaon. A vertex fit is performed that constrains the three daughter particles to originate from a common point and the mass of the muon pair to match the nominal J/ψ mass. It is required that $\chi^2/\text{ndf} < 9$ for this fit. To further reduce the combinatorial background due to particles produced in the primary pp interaction, only candidates with a decay time larger than 0.3 ps are accepted. Finally, the fiducial requirement $0 < p_T < 40 \text{ GeV}/c$ and $2.0 < y < 4.5$ is applied to the B^\pm candidates.

3 Cross-section determination

The differential production cross-section is measured as

$$\frac{d\sigma}{dp_T} = \frac{N_{B^\pm}(p_T)}{\mathcal{L} \varepsilon_{\text{tot}}(p_T) \mathcal{B}(B^\pm \rightarrow J/\psi K^\pm) \mathcal{B}(J/\psi \rightarrow \mu^+ \mu^-) \Delta p_T}, \quad (1)$$

where $N_{B^\pm}(p_T)$ is the number of reconstructed $B^\pm \rightarrow J/\psi K^\pm$ signal events in a given p_T bin, \mathcal{L} is the integrated luminosity, $\varepsilon_{\text{tot}}(p_T)$ is the total efficiency, including geometrical acceptance, reconstruction, selection and trigger effects, $\mathcal{B}(B^\pm \rightarrow J/\psi K^\pm)$ and $\mathcal{B}(J/\psi \rightarrow \mu^+ \mu^-)$ are the branching fractions of the reconstructed decay chain [10], and Δp_T is the p_T bin width.

Considering that the efficiencies depend on p_T and y , we calculate the event yield in bins of these variables using an extended unbinned maximum likelihood fit to the invariant mass distribution of the reconstructed B^\pm candidates in the interval $5.15 < M_{B^\pm} < 5.55 \text{ GeV}/c^2$. We assume that the signal and background shapes only depend on p_T . Three components are included in the fit procedure: a Crystal Ball function [11] to model the signal, an exponential function to model the combinatorial background and a double-Crystal Ball function¹ to model the Cabibbo suppressed decay $B^\pm \rightarrow J/\psi \pi^\pm$. The shape of the latter component is found to fit well the distribution of simulated events. The ratio of the number of $B^\pm \rightarrow J/\psi \pi^\pm$ candidates to that of the signal is fixed to $\mathcal{B}(B^\pm \rightarrow J/\psi \pi^\pm)/\mathcal{B}(B^\pm \rightarrow J/\psi K^\pm)$ from Ref. [10]. The invariant mass distribution of the selected $B^\pm \rightarrow J/\psi K^\pm$ candidates and the fit result for one bin

¹A double-Crystal Ball function has tails on both the low and high mass side of the peak with separate parameters for the two.

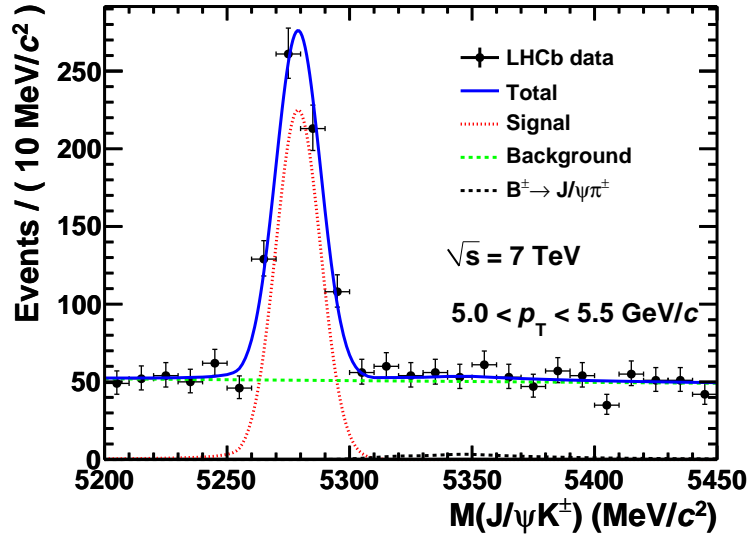


Figure 1: Invariant mass distribution of the selected $B^\pm \rightarrow J/\psi K^\pm$ candidates for one bin ($5.0 < p_T < 5.5 \text{ GeV}/c$). The result of the fit to the model described in the text is superimposed.

($5.0 < p_T < 5.5 \text{ GeV}/c$) are shown in Fig. 1. The fit returns a mass resolution of $9.14 \pm 0.49 \text{ MeV}/c^2$, and a mean of $5279.05 \pm 0.56 \text{ MeV}/c^2$, where the uncertainties are statistical only. Summing over all p_T bins, the total number of signal events is about 9100.

The geometrical acceptance and the reconstruction and selection efficiencies are determined using simulated signal events. The simulation is based on PYTHIA 6.4 generator [12] with parameters configured for LHCb [13]. The EVTGEN package [14] is used to describe the decays of the B^\pm and J/ψ . QED radiative corrections are modelled using PHOTOS [15]. The GEANT4 [16] simulation package is used to trace the decay products through the detector. Since we select events passing trigger selections that depend on J/ψ properties only, the trigger efficiency is obtained from a trigger-unbiased data sample of J/ψ events that would still be triggered if the J/ψ candidate were removed. The efficiency of GEC is determined from data to be $(92.6 \pm 0.3)\%$, and assumed to be independent of the B^\pm p_T and y . The total trigger efficiency is then the product of the J/ψ trigger efficiency and the GEC efficiency. The luminosity is measured using Van der Meer scans and a beam-gas imaging method [17]. The knowledge of the absolute luminosity scale is used to calibrate the number of tracks in the vertex detector, which is found to be stable throughout the data-taking period and can therefore be used to monitor the instantaneous luminosity of the entire data sample. The integrated luminosity of the data sample used in this analysis is determined to be 34.6 pb^{-1} .

The measurement is affected by the systematic uncertainty on the determination of signal yields, efficiencies, branching fractions and luminosity.

The uncertainty on the determination of the signal yields mainly arises from the description of final state radiation in the signal fit. The fitted signal yield is corrected by 3.0%, which is estimated by comparing the fitted and generated signal yields in the Monte Carlo simulation, and an uncertainty of 1.5% is assigned. The uncertainties from the effects of the Cabibbo-

suppressed background, multiple candidates and mass fit range are found to be negligible.

The uncertainties on the efficiencies arise from trigger (0.5 – 6.0% depending on the bin), tracking (3.9 – 4.4% depending on the bin), muon identification (2.5%) [5] and the vertex fit quality cut (1.0%). The trigger systematic uncertainty has been evaluated by measuring the trigger efficiency in the simulation using a trigger-unbiased data sample of simulated J/ψ events. The tracking uncertainty includes two components: the first one is the differences in track reconstruction efficiency between data and simulation, estimated with a tag and probe method [18] using $J/\psi \rightarrow \mu^+ \mu^-$ events; the second is due to the 2% uncertainty on the hadronic interaction length of the detector used in the simulation. The uncertainties from the effects of GEC, J/ψ mass window cut and inter-bin cross-feed are found to be negligible. The uncertainty due to the choice of p_T binning is estimated to be smaller than 2.0%.

The product of $\mathcal{B}(B^\pm \rightarrow J/\psi K^\pm)$ and $\mathcal{B}(J/\psi \rightarrow \mu^+ \mu^-)$ is calculated to be $(6.01 \pm 0.20) \times 10^{-5}$, by taking their values from Ref. [10] with their correlations taken into account.

The absolute luminosity scale is measured with a 3.5% uncertainty [17], dominated by the beam current uncertainty.

4 Results and conclusion

The measured B^\pm differential production cross-section in bins of p_T for $2.0 < y < 4.5$ is given in Table 1. This result is compared with a FONLL prediction [2, 3] in Fig. 2. A hadronisation fraction $f_{\bar{b} \rightarrow B^+}$ of $(40.1 \pm 1.3)\%$ [10] is assumed to fix the overall scale of FONLL. The uncertainty of the FONLL computation includes the uncertainties on the b -quark mass, renormalisation and factorisation scales, and CTEQ 6.6 [19] Parton Density Functions (PDF). Good agreement is observed between data and the FONLL prediction. The integrated cross-section is

$$\sigma(pp \rightarrow B^\pm X, 0 < p_T < 40 \text{ GeV}/c, 2.0 < y < 4.5) = 41.4 \pm 1.5 (\text{stat.}) \pm 3.1 (\text{syst.}) \mu\text{b}.$$

This is the first measurement of B^\pm production in the forward region at $\sqrt{s} = 7 \text{ TeV}$.

Acknowledgements

We express our gratitude to our colleagues in the CERN accelerator departments for the excellent performance of the LHC. We thank the technical and administrative staff at CERN and at the LHCb institutes, and acknowledge support from the National Agencies: CAPES, CNPq, FAPERJ and FINEP (Brazil); CERN; NSFC (China); CNRS/IN2P3 (France); BMBF, DFG, HGF and MPG (Germany); SFI (Ireland); INFN (Italy); FOM and NWO (The Netherlands); SCSR (Poland); ANCS (Romania); MinES of Russia and Rosatom (Russia); MICINN, XuntaGal and GENCAT (Spain); SNSF and SER (Switzerland); NAS Ukraine (Ukraine); STFC (United Kingdom); NSF (USA). We also acknowledge the support received from the ERC under FP7 and the Region Auvergne.

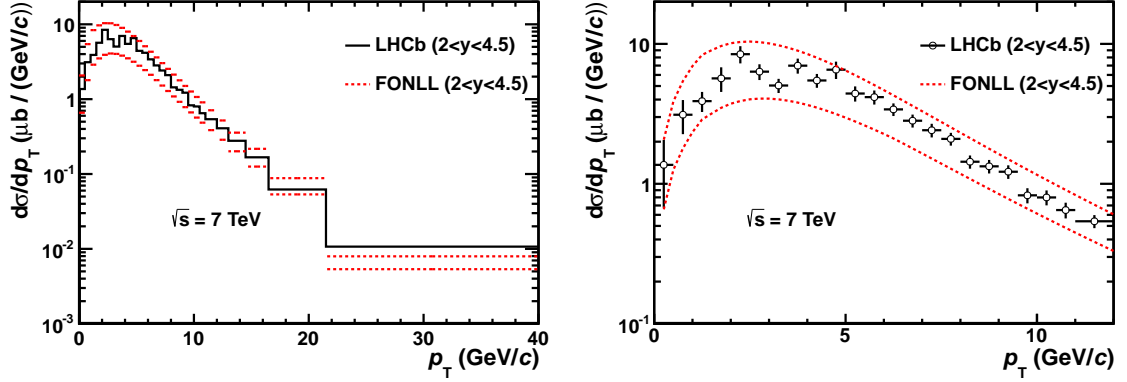


Figure 2: Differential production cross-section as a function of the B^\pm transverse momentum. The left plot shows the full p_T range, the right plot shows a zoom of the p_T range of 0 – 12 GeV/ c . The histogram (left) and the open circles with error bars (right) are the measurements. The red dashed lines in both plots are the upper and lower uncertainty limits of the FONLL computation. A hadronisation fraction $f_{\bar{b} \rightarrow B^+}$ of $(40.1 \pm 1.3)\%$ [10] is assumed to fix the overall scale. The uncertainty of the FONLL computation includes the uncertainties of the b -quark mass, renormalisation and factorisation scales, and CTEQ 6.6 PDF.

Table 1: Differential B^\pm production cross-section in bins of p_T for $2.0 < y < 4.5$. The first and second quoted uncertainties are statistical and systematic, respectively.

p_T (GeV/ c)	$d\sigma/dp_T$ ($\mu\text{b}/(\text{GeV}/c)$)	p_T (GeV/ c)	$d\sigma/dp_T$ ($\mu\text{b}/(\text{GeV}/c)$)
0.0 – 0.5	$1.37 \pm 0.68 \pm 0.13$	7.0 – 7.5	$2.42 \pm 0.20 \pm 0.18$
0.5 – 1.0	$3.12 \pm 0.82 \pm 0.24$	7.5 – 8.0	$2.09 \pm 0.16 \pm 0.15$
1.0 – 1.5	$3.90 \pm 0.57 \pm 0.29$	8.0 – 8.5	$1.44 \pm 0.11 \pm 0.11$
1.5 – 2.0	$5.67 \pm 1.05 \pm 0.43$	8.5 – 9.0	$1.33 \pm 0.11 \pm 0.10$
2.0 – 2.5	$8.44 \pm 1.00 \pm 0.64$	9.0 – 9.5	$1.22 \pm 0.10 \pm 0.09$
2.5 – 3.0	$6.33 \pm 0.66 \pm 0.48$	9.5 – 10.0	$0.83 \pm 0.08 \pm 0.06$
3.0 – 3.5	$5.04 \pm 0.45 \pm 0.38$	10.0 – 10.5	$0.80 \pm 0.08 \pm 0.06$
3.5 – 4.0	$6.99 \pm 0.68 \pm 0.52$	10.5 – 11.0	$0.65 \pm 0.07 \pm 0.05$
4.0 – 4.5	$5.48 \pm 0.47 \pm 0.41$	11.0 – 12.0	$0.54 \pm 0.04 \pm 0.04$
4.5 – 5.0	$6.54 \pm 0.79 \pm 0.49$	12.0 – 13.0	$0.41 \pm 0.04 \pm 0.03$
5.0 – 5.5	$4.42 \pm 0.44 \pm 0.33$	13.0 – 14.5	$0.28 \pm 0.02 \pm 0.02$
5.5 – 6.0	$4.16 \pm 0.37 \pm 0.31$	14.5 – 16.5	$0.17 \pm 0.02 \pm 0.01$
6.0 – 6.5	$3.40 \pm 0.24 \pm 0.25$	16.5 – 21.5	$0.062 \pm 0.005 \pm 0.005$
6.5 – 7.0	$2.82 \pm 0.22 \pm 0.21$	21.5 – 40.0	$0.011 \pm 0.001 \pm 0.001$

References

- [1] P. Nason, S. Dawson, and R. K. Ellis, *The total cross-section for the production of heavy quarks in hadronic collisions*, Nucl. Phys. **B303** (1988) 607.
- [2] M. Cacciari, M. Greco, and P. Nason, *The p_T spectrum in heavy flavor hadroproduction*, JHEP **05** (1998) 007, arXiv:hep-ph/9803400.
- [3] M. Cacciari, S. Frixione, and P. Nason, *The p_T spectrum in heavy flavor photoproduction*, JHEP **03** (2001) 006, arXiv:hep-ph/0102134.
- [4] M. Cacciari *et al.*, *QCD analysis of first b cross-section data at 1.96 TeV*, JHEP **07** (2004) 033, arXiv:hep-ph/0312132.
- [5] LHCb collaboration, R. Aaij *et al.*, *Measurement of J/ψ production in pp collisions at $\sqrt{s}=7$ TeV*, Eur. Phys. J. **C71** (2011) 1645, arXiv:1103.0423.
- [6] LHCb collaboration, R. Aaij *et al.*, *Measurement of $\sigma(pp \rightarrow b\bar{b}X)$ at $\sqrt{s} = 7$ TeV in the forward region*, Phys. Lett. **B694** (2010) 209, arXiv:1009.2731.
- [7] CDF collaboration, A. Abulencia *et al.*, *Measurement of the B^+ production cross-section in $p\bar{p}$ collisions at $\sqrt{s} = 1960$ GeV*, Phys. Rev. **D75** (2007) 012010, arXiv:hep-ex/0612015.
- [8] CMS collaboration, V. Khachatryan *et al.*, *Measurement of the B^+ production cross section in pp Collisions at $\sqrt{s} = 7$ TeV*, Phys. Rev. Lett. **106** (2011) 112001, arXiv:1101.0131.
- [9] LHCb collaboration, A. A. Alves Jr. *et al.*, *The LHCb detector at the LHC*, JINST **3** (2008) S08005.
- [10] Particle Data Group, K. Nakamura *et al.*, *Review of particle physics*, J. Phys. **G37** (2010) 075021.
- [11] T. Skwarnicki, *A study of the radiative cascade transitions between the Υ' and Υ resonances*, Ph.D. Thesis, DESY-F31-86-02 (1986).
- [12] T. Sjöstrand, S. Mrenna, and P. Skands, *PYTHIA 6.4 physics and manual*, JHEP **05** (2006) 026, arXiv:hep-ph/0603175.
- [13] M. Clemencic *et al.*, *The LHCb Simulation Application, Gauss: Design, Evolution and Experience*, Journal of Physics: Conference Series **331** (2011), no. 3 032023.
- [14] D. J. Lange, *The EVTGEN particle decay simulation package*, Nucl. Instrum. Methods **A462** (2001) 152.
- [15] P. Golonka and Z. Was, *PHOTOS Monte Carlo: A precision tool for QED corrections in Z and W decays*, Eur. Phys. J. **C45** (2006) 97, arXiv:hep-ph/0506026.

- [16] GEANT4 collaboration, S. Agostinelli *et al.*, *GEANT4: a simulation toolkit*, Nucl. Instrum. Methods **A506** (2003) 250.
- [17] LHCb collaboration, R. Aaij *et al.*, *Absolute luminosity measurements with the LHCb detector at the LHC*, JINST **7** (2012) P01010, arXiv:1110.2866.
- [18] LHCb collaboration, R. Aaij *et al.*, *Prompt K_s^0 production in pp collisions at $\sqrt{s} = 0.9$ TeV*, Phys. Lett. **B693** (2010) 69, arXiv:1008.3105.
- [19] P. M. Nadolsky *et al.*, *Implications of CTEQ global analysis for collider observables*, Phys. Rev. **D78** (2008) 013004, arXiv:0802.0007.